South African Journal of Chemical Engineering 45 (2023) 60–72

Contents lists available at ScienceDirect

South African Journal of Chemical Engineering

journal homepage: www.elsevier.com/locate/sajce

Dolomite catalyst for fast pyrolysis of waste cooking oil into hydrocarbon fuel

Yorinda Buyang [a,b], Reva Edra Nugraha [c], Holilah Holilah [d], Hasliza Bahruji [e], Suprapto Suprapto [a], Aishah Abdul Jalil [f,g], Muryani Muryani [h], Didik Prasetyoko [a,*]

[a] Department of Chemistry, Faculty of Science and Data Analytics, Institut Teknologi Sepuluh Nopember, Keputih, Sukolilo, Surabaya, 60111, Indonesia
[b] Department of Chemistry Education, Faculty of Teacher Training and Education, Musamus University, Merauke, Papua, 99600, Indonesia
[c] Department of Chemical Engineering, Faculty of Engineering, Universitas Pembangunan Nasional "Veteran" Jawa Timur, Surabaya, 60294, Indonesia
[d] Research Center for Biomass and Bioproducts, National Research and Innovation Agency of Indonesia (BRIN), Cibinong, 16911, Indonesia
[e] Centre of Advanced Material and Energy Sciences, Universiti Brunei Darussalam, Jalan Tungku Link, BE 1410, Brunei
[f] Department of Chemical Engineering, Faculty of Chemical and Energy Engineering, Universiti Teknologi Malaysia, 81310 UTM, Skudai, Johor Bahru, Johor, Malaysia
[g] Centre of Hydrogen Energy, Institute of Future Energy, Universiti Teknologi Malaysia, Skudai, Johor Bahru, Johor, 81310, Malaysia
[h] Department of Municipal Waste, Blitar District, East Java, Indonesia

ARTICLE INFO

Keywords:
Bio-oil
Catalytic fast pyrolysis
Dolomite
Hydrocarbon
Waste cooking oil

ABSTRACT

Dolomite as the catalyst for pyrolysis of waste cooking oil (WCO) was investigated to produce hydrocarbon fuels. Optimization of pyrolysis parameters i.e. time, temperature and catalysts loading, achieved high selectivity of WCO to diesel hydrocarbon, compared to thermal pyrolysis that produced mainly carboxylic acids. Dolomite catalysed deoxygenation of fatty acid in WCO into hydrocarbon, consequently accelerating the pyrolysis time to 75 min. Bio-oil at 68.06% yield with 57.27% selectivity towards diesel and gasoline hydrocarbons was obtained at 450 °C while using 6% of dolomite. Dolomite exhibited partial phase separation into dolomite/$CaCO_3$ mixtures within 15 min of pyrolysis, initiated by the generated CO_2 during pyrolisis of WCO. The catalyst is stable for up to three reaction cycles suggesting the activity was achieved from the synergy between the dolomite/$CaCO_3$ phases.

1. Introduction

The depletion of crude oil reserves and the fluctuation of oil prices prompted research on sustainable and renewable energy (Raman et al., 2018). Biomass upgrading into fuel is a potential way to generate renewable energy from abundant carbon reserves (Luo et al., 2022). Biomass as a renewable energy source can supply two-thirds of the total global energy demand and reduce greenhouse gas emissions by 2050 (Gielen et al., 2019). Waste oil such as soap stock, engine oil waste, clay oil, and waste cooking oil (WCO) can be converted to renewable fuel. Waste oil has a higher volatile organic compound than cellulose-based biomass and generally produces a high bio-oil yield (Su et al., 2022). Waste cooking oil consists of at least 95% triglycerides with long-chain fatty acids such as stearic acid (C18) and palmitic acid (C16), and therefore it is in great demand for conversion to fuel (Kassa et al., 2022; Wu et al., 2022). Upgrading the waste oil via pyrolysis into fuel will have a big impact on the future energy industry. Advanced pyrolysis provides a solid platform for the environmentally responsible treatment of waste oil. The efforts to reduce the culmination of waste oil by upgrading to valuable products are aligned with the circular economy guideline (Su et al., 2022).

Pyrolysis is an endothermic decomposition process carried out in an oxygen-free environment at high temperatures producing liquid bio-oil, bio-char, and gasses (Zhang et al., 2014). Pyrolysis of biomass provides a facile method for generating fuels and chemicals from renewable resources (Norouzi et al., 2021; Ben Hassen Trabelsi et al., 2018). Pyrolysis offers flexibility in operation throughout a wide temperature range and air pressure, converting waste oil into high-quality biofuels (Melia et al., 2021). Biofuels are being marketed as low-carbon substitutes for fossil fuels to reduce greenhouse gas (GHG) emissions and to minimize the associated impact of transportation on climate change (Su et al., 2022; Jeswani et al., 2020). On the other hand, the disposal techniques for waste oil such as gasification, transesterification, hydrotreating, solvent extraction, and membrane technology struggle to achieve satisfactory

* Corresponding author.
E-mail address: didikp@chem.its.ac.id (D. Prasetyoko).

https://doi.org/10.1016/j.sajce.2023.04.007
Received 4 December 2022; Received in revised form 13 March 2023; Accepted 20 April 2023
Available online 22 April 2023

results due to high processing energy and times that contributed to higher operating costs, and also the generation of hazardous pollution from the processes (Su et al., 2022).

Bio-oil containing olefin and aromatic compounds can be obtained through fast pyrolysis of biomass (Valle et al., 2019). Pyrolysis can produce up to 70% of the liquid bio-oil yield from biomass feedstock (Galadima and Muraza, 2015; Ge et al., 2022). However, the application of bio-oils as fuel is restricted by the low thermal stability, low volatility, high acidity and low calorific value (Dai et al., 2019). The properties of bio-oil were improved with the subsequent treatment through catalytic cracking (Ibarra et al., 2019), esterification (Zhang et al., 2015), photo-enzymatic (Guo et al., 2022) and hydro-conversion (Kang et al., 2021). The relationships between the structure and functionality of the catalyst determine the conversion, product selectivity, and catalytic lifetime, hence propelling the advancements of heterogeneous catalysis (Ruddy et al., 2014; Fadillah et al., 2021). It is necessary to develop a low-cost catalyst to ensure the economic viability of waste oil conversion into bio-oil (Fadillah et al., 2021). Biocatalysts and inorganic catalysts have been widely employed to improve catalytic pyrolysis performance. However, biocatalyst performance is hampered by a slow reaction rate and poor stability due to enzyme deactivation (Nayab et al., 2022). Inorganic acid catalysts such as zeolite Y (Kassa et al., 2022), ZSM-5 (Long et al., 2020), MCM-41 (Wang et al., 2021) and SBA-15 (Miro De Medeiros et al., 2022) improved the bio-oil quality. In addition, base catalysts, including CaO (Wu et al., 2022), MgO (Prasad et al., 2022), Na_2CO_3 (Hatefirad and Tavasoli, 2021), and K_2CO_3 (Wang et al., 2021) have been used in pyrolysis to reduce acids and increase hydrocarbon yield. In catalytic pyrolysis, acid catalyst displays significant activity in the aromatization and reduction of oxygenated molecules, while base catalysts facilitated the deacidification of bio-oil from biomass (Melia et al., 2021). In recent years, the use of calcium-based minerals as a base catalyst has been actively developed mainly due to their high catalytic performance and low prices (Li et al., 2021).

Dolomite ($CaMg(CO_3)_2$) mineral was used as the catalyst for the pyrolysis of municipal solid waste and grass into syngas (H_2 + CO) (Conesa and Domene, 2015). Gao et al., (2019) reported that dolomite reduced sulfur content in coal pyrolysis, while others reported dolomite activity in reducing tar content during pyrolysis (Berrueco et al., 2014; Shien et al., 2019; Wang and Shen, 2022). The use of calcined dolomite in the catalytic gasification of rice husks increased the gas yield from 1.23 to 1.42 Nm^3/kg and reduced the tar yield from 15.2 to 1.8 Nm^3/kg (Zhang et al., 2018). Modification of calcined dolomite with Ni nanoparticles and $MgCO_3$ enhanced the pyrolysis of WCO (Hafriz et al., 2021; Kanchanatip et al., 2022). Calcination of dolomite produced CaO/MgO base catalysts that enhanced the deoxygenation and cracking of heavy compounds into lighter hydrocarbon fractions, and reduced char formation (Ly et al., 2018; Valle et al., 2019). CaO/MgO was reported to remove the acidity of pyrolytic oil and increase the concentration of methyl phenol and methyl cyclopentanone on rapid pyrolysis of beech wood (Mysore Prabhakara et al., 2021). Moreover, dolomite is also reported to have high CO_2 adsorption potential that can be employed to simultaneously reduced CO_2 emission (Tao et al., 2021).

In this study, fresh dolomite (FD) was investigated as the catalyst for the catalytic pyrolysis of WCO. Comparative studies were conducted on thermal pyrolysis in the absence of catalysts, and when using calcined dolomite to elucidate the superior role of dolomite to enhance liquid bio-oil formation and to increase hydrocarbon selectivity. The activity and stability of dolomite were investigated by varying reaction times and reaction cycles. Most of the reported studies revealed that calcined dolomite exhibited high activity for the pyrolysis of various types of biomasses. This study observed high catalytic activity of fresh dolomite than the calcined dolomite due to the partial separation of dolomite into dolomite/$CaCO_3$ phases. Monitoring the structural changes of fresh dolomite during the pyrolysis of WCO and its bio-oil composition will be beneficial in generating a high-quality bio-oil while employing a minimum step for catalyst activation.

2. Experimental

2.1. Materials

The waste cooking oil (WCO) was collected from households in Surabaya, Indonesia. The feedstock is filtered to separate the frying residue contained in the oil. Dolomite was collected from Madura, East Java, Indonesia. The dolomite was grounded and sieved to get the uniform particles at approximately 80 mesh. The sieved dolomite was dried in an oven at 105 °C for 24 h. In addition, calcined dolomite was obtained by annealing at 850 °C for 4 h under air to form CaO/MgO phase.

2.2. Characterization of feedstock

The fatty acid composition of WCO was studied using gas chromatography-mass spectroscopy (HP 6890 GC) with capillary column HP-5MS (length: 30 mx inner diameter: 0.25 mm x film thickness: 0.25 μm). The GCMS inlet temperature was kept at 250 °C, and the oven was programmed at 65 °C for 8 min. The temperature was slowly increased at 4 °C/min heating rate to reach 250 °C and maintained at 250 °C for 15 min. The ion source temperature was set at 200 °C. The weight loss of WCO was determined using Hitachi STA7200 thermogravimetric analyzer, at 30–600 °C under N_2 conditions.

2.3. Characterization of catalyst

Dolomite and calcined dolomite were characterized using Fourier Transform Infrared (FTIR), Shimadzu Instrument Spectrum one 8400S and X-ray Diffraction (XRD) PHILIPS-binary XPert with MPD diffractometer with Cu Kα radiation operated at 30 mA and 40 kV. The textural properties were analyzed using Quantachrome instruments version 11.0. The surface area was calculated using Brunauer Emmet Teller (BET), and the pore size distribution was calculated by Barett Joyner Halenda (BJH) methods. The morphology and the elemental analysis of dolomite were analyzed using Hitachi Scanning Electron Microscope Flex SEM 1000 combined with energy dispersive X-ray spectroscopy (EDX).

2.4. Pyrolysis of WCO

The homemade semi-batch reactor used for the pyrolysis of WCO and the bio-oil products is shown in Fig. 1. The reactor consisted of a stainless-steel chamber (dimensions: 61 cm long and 59 cm wide) with 10 L of total volume capacity. The thermal pyrolysis temperature was varied at 350, 450 and 550 °C, while the catalytic pyrolysis was conducted at 450 °C. A total of 1500 g of WCO was poured into a stainless chamber reactor for thermal pyrolysis, and the reaction was carried out to achieve 100% conversion of WCO. The complete decomposition of WCO was achieved when no more liquid or gasses produced from the pyrolysis reactor. For catalytic pyrolysis, the amount of catalyst loading was varied at 1, 3 and 6% relative to the total WCO feedstock. Dolomite was dried in an oven at 105 °C for 24 h before being mixed with WCO. The mixture of WCO and dolomite is poured into the chamber through the feedstock inlet (Fig. 1: part 1 and 2). The reaction was carried out at 450 °C at atmospheric pressure. Liquid bio-oil yield collected from outlet 4 is labeled as L1, liquid yield from outlet 5 is labeled as L2 and liquid yield from outlet 6 is labeled as L3 (Fig. 1). The acquisition times for L1-L3 are different, in which L1 is collected first followed by L2 and L3. Nevertheless, the liquid yield collected from all outlets was mixed before GCMS and FTIR analysis. The pyrolytic oil produced from non-catalytic pyrolysis was labeled as 0%FD, while the oil from catalytic pyrolysis using 1%, 3% and 6% of fresh dolomite loading, were labeled as 1%FD, 3%FD and 6%FD, respectively. The non-condensable gas is removed from outlet 8. The pyrolysis temperature was monitored using a thermocouple installed in the reactor in part 9 and the heating stove in part 3 (Fig. 1). The bio-oil yield and solid residue were calculated after the

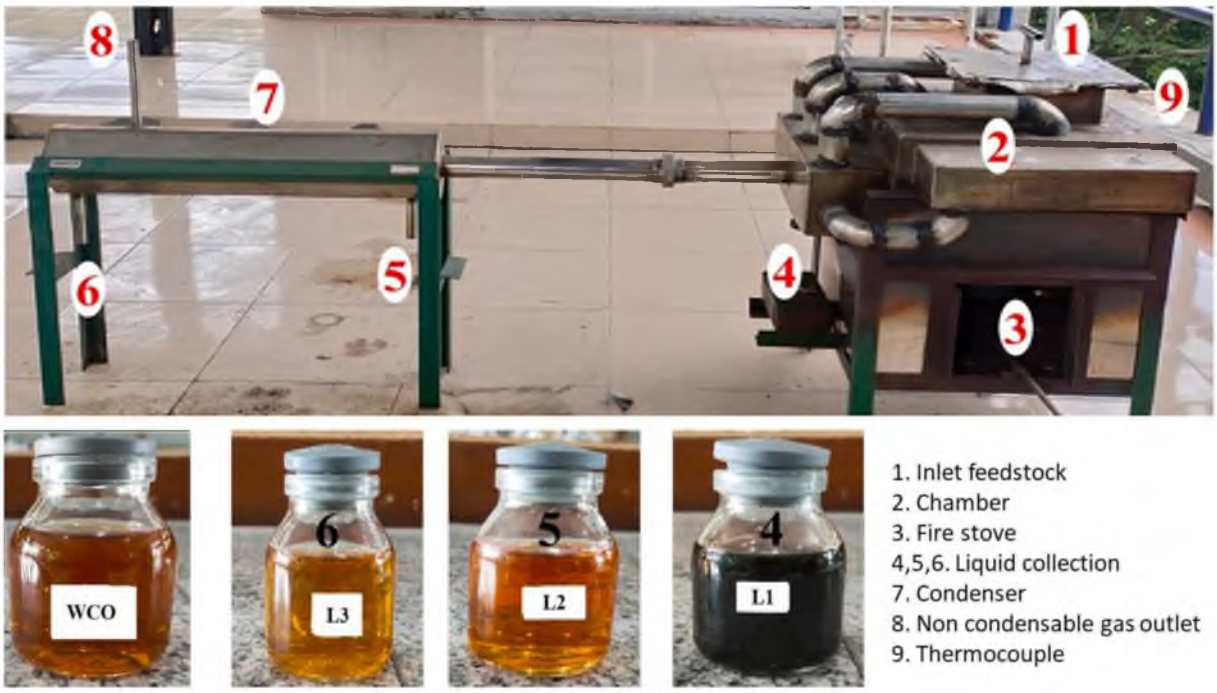

Fig. 1. The image of homemade semi batch reactor, WCO feedstock and the liquid yield from pyrolysis of WCO.

pyrolysis achieved 100% conversion, which varied depending on the amount of dolomite loading. The effect of pyrolysis time was conducted using 1500 g of WCO and 6% fresh dolomite (FD) catalyst at 15, 30, 45, 60 and 75 min.

2.5. Characterization of bio-oil and bio-char

The bio-oil obtained from the pyrolysis of WCO is analyzed using GCMS HP 6890 GC with HP-5MS capillary column (length: 30 mm inner diameter: 0.25 mm x film thickness: 0.25 μm). The GCMS inlet temperature was kept at 250 °C, and the oven was programmed at 65 °C for 8 min. The temperature was slowly increased at 4 °C/min heating rate to reach 250 °C and maintained at 250 °C for 15 min. The ion source temperature was set at 200 °C. 1-bromohexane was used as an internal standard for the quantitative analysis. The bio-char obtained was characterized using a wide -angle X-ray Diffraction (XRD) PHILIPS-binary XPert with MPD diffractometer with Cu Kα radiation operated at 30 mA and 40 kV. The yield of each pyrolysis product and selectivity was calculated by Eqs. ((1)-(4)):

$$Liquid\ yield\ (\%) = \frac{weight\ of\ bio-oil}{weight\ feedstock} x100 \quad (1)$$

$$Char\ yield\ (\%) = \frac{weight\ of\ char}{weight\ of\ feedstock} x100 \quad (2)$$

$$\text{Gas yield } (\%) = 100 - (\text{oil yield} + \text{char yield}) \quad (3)$$

$$\text{Selectivity} = \frac{\text{Weight of component Ha}}{\sum \text{weight of all component}} \text{x100} \quad (4)$$

Ha: specific compounds of hydrocarbons

3. Result and discussion

3.1. Characterization of waste cooking oil (WCO)

TG/DTG measures the mass loss as a function of temperature that offers information on the thermal stability and decomposition temperature of WCO (Sharma et al., 2021). The TG/DTG result in Fig. 2 showed

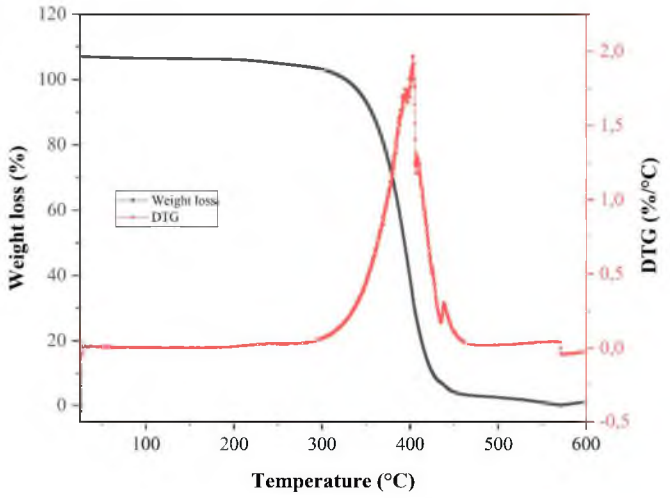

Fig. 2. TGA/DTG profiles of WCO.

a gradual weight loss of ~5% when the temperature was increased up to 320 °C due to the evacuation of water and volatile compounds in WCO. The breakdown of monounsaturated and polyunsaturated fatty acids in WCO occurred at 320–472 °C resulted in 96.73% of weight loss (Zhou et al., 2022). Table 1 summarized the fatty acid composition of the WCO used in this study which was determined using GCMS analysis. The WCO contains a series of C12:0 to C20:3 fatty acid compounds with oleic acid (C18:1) as the main compound at 40.02%, followed by palmitic acid (C16:0) at 34.72%. Considerable amounts of stearic acid, linoleic acid, and eicosatrienoic acid were also detected in which the composition of WCO was similar to the previous study (Shen et al., 2019). The composition of fatty acid has a significant effect on the hydrocarbon structures. Waste cooking oil with long fatty acids such as oleic acid and palmitic acid will have the potential to produce hydrocarbon fuel. Identification of the main components in WCO and the pyrolytic oil composition will provide insight into the mechanism of the reaction.

Table 1
Fatty acid in triglycerides of studied in WCO.

Fatty acids composition	Molecular formula	Content (wt.%) This study	Previous study (Shen et al., 2019)
Lauric acid (C12:0)	$C_{12}H_{24}O_2$	0.40	–
Myristic acid (C14:0)	$C_{14}H_{28}O_2$	1.06	0.52
Palmitic acid (C16:0)	$C_{16}H_{32}O_2$	34.72	16.32
Palmitoleic acid (C16:1)	$C_{16}H_{30}O_2$	0.53	–
Stearic acid (C18:0)	$C_{18}H_{36}O_2$	4.75	8.21
Oleic acid (C18:1)	$C_{18}H_{34}O_2$	40.02	40.24
Linoleic acid (C18:2)	$C_{18}H_{32}O2$	12.49	28.35
Eicosatrienoic acid (C20:3)	$C_{20}H_{34}O_2$	1.30	–
Arachidic acid (C20:0)	$C_{20}H_{40}O_2$	0.35	–
Alkane	C_nH_{2n+2}	3.54	5.14

3.2. Characterization of catalyst

The XRD analysis of dolomite in Fig. 3a shows all the peaks corresponding to the dolomite mineral supported by ICDD card # 10–036–0426. Calcined dolomite showed the formation of $CaCO_3$, CaO and MgO. The high intense peaks of $CaCO_3$ (ICDD card # 00–047–1743) appeared at 2θ = 23.05, 29.39, 36.0, 39.36, 47.53 and 48.47° Meanwhile, weak diffraction peaks of CaO (ICDD card # 00–003–1123) and MgO (ICDD card # 00–002–1207) were observed at 2θ = 32.27° and 37.24° and 2θ= 36.97°, 42.91° and 62.28° Thermal decomposition of dolomite to CaO/MgO follows two-stage processes that involve the decomposition of dolomite into $CaCO_3$ and MgO (I) at 550–765 °C, and the decomposition of $CaCO_3$ into CaO (II) at >900 °C (Olszak-Humienik and Jablonski, 2014; Maitra et al., 2005). Calcium carbonate dissociation into the extremely reactive calcium oxide occurs during the second stage of the dolomite decomposition. The process is reversible, in which calcium oxide can be carbonated and hydroxylated with carbon dioxide and moisture from the air to form $CaCO_3$, causing a weak peak of CaO in XRD analysis.

$$CaMg(CO_3)_2 \leftrightarrow CaCO_3 + MgO + CO_2 \quad (5)$$

$$CaCO_3 \leftrightarrow CaO + CO_2 \quad (6)$$

Powder XRD analysis was also conducted on the dolomite catalyst recovered after the reaction which revealed a mixture of dolomite and calcium carbonate (Fig. 3b). The dolomite phase appeared at 2θ: 24.00, 31.06, 33.46, 37.40, 41.35, 45.07. 50.55 and 51.20, while the calcium carbonate phase was observed at 2θ: 23.30, 29.43, 36.25, 39.60, 43.36, 47.53, and 48.65. The XRD analysis also showed evidence of carbon char formation. The XRD analysis of solid residue from thermal pyrolysis without dolomite showed a broad diffraction peak at 2θ = 20–30° which corresponds to carbonaceous char (Zhu et al., 2020). Char deposit was also observed when using 1% of fresh dolomite (1%FD). No discernible carbon char residue was observed on the recovered solid from 3%FD and 6%FD, which indicates dolomite inhibits char formation during catalytic pyrolysis of WCO. Despite all the dolomite peaks being preserved after pyrolysis, peaks corresponding to calcium carbonate were observed regardless of catalyst concentrations. Nevertheless, calcium carbonate concentration on the spent catalyst was lower with increasing the loading of the catalyst.

Calcined dolomite formed CaO/MgO mixtures that offer synergy towards pyrolysis reaction. MgO reduced the acid composition of bio-oil through ketonization and condensation aldol (B. Valle et al., 2019), while CaO catalyzed the decarboxylation reaction to form hydrocarbon (X. Chen et al., 2019). The deoxygenation of hydroxyl, carbonyl and carboxyl compounds occurred on CaO, which leads to the formation of aliphatic hydrocarbons (Wu et al., 2022). MgO was reported to catalyze the decomposition of volatile macromolecular compounds and prevent the deactivation of CaO active sites caused by char formation (Islam, 2020). Charusiri, 2017 reported that CaO and MgO were very effective in removing carboxyl and carbonyl groups from bio-oil (Charusiri and Vitidsant, 2017). However, the synergy between CaO and MgO reduced the formation of carbon from aliphatic hydrocarbons and produced more volatiles into non-condensable gasses (Pütün, 2010). The basicity of CaO/MgO also tends to capture CO_2 which leads to the formation of $CaCO_3$ and bio-char (Valle et al., 2020).

The FTIR analysis of dolomite in Fig. 4 shows the absorption bands at 722, 874, 1446 and 3471 cm^{-1} (Susianti et al., 2022). In general, the strong bands at 722, 874 and 1446 cm^{-1} exhibited the in-plane bending, out-of-plane bending, and asymmetric stretching of CO_3^{2-}, respectively (Wang, 2019; T. Chen et al., 2019). The absorption band at 722 cm^{-1} is a typical characteristic of dolomite (Ji et al., 2009). The presence of water is indicated by the hydroxyl band at 3471 cm^{-1}. Similar absorption bands were observed on calcined dolomite at 874, 1067, 1425, 3467 and

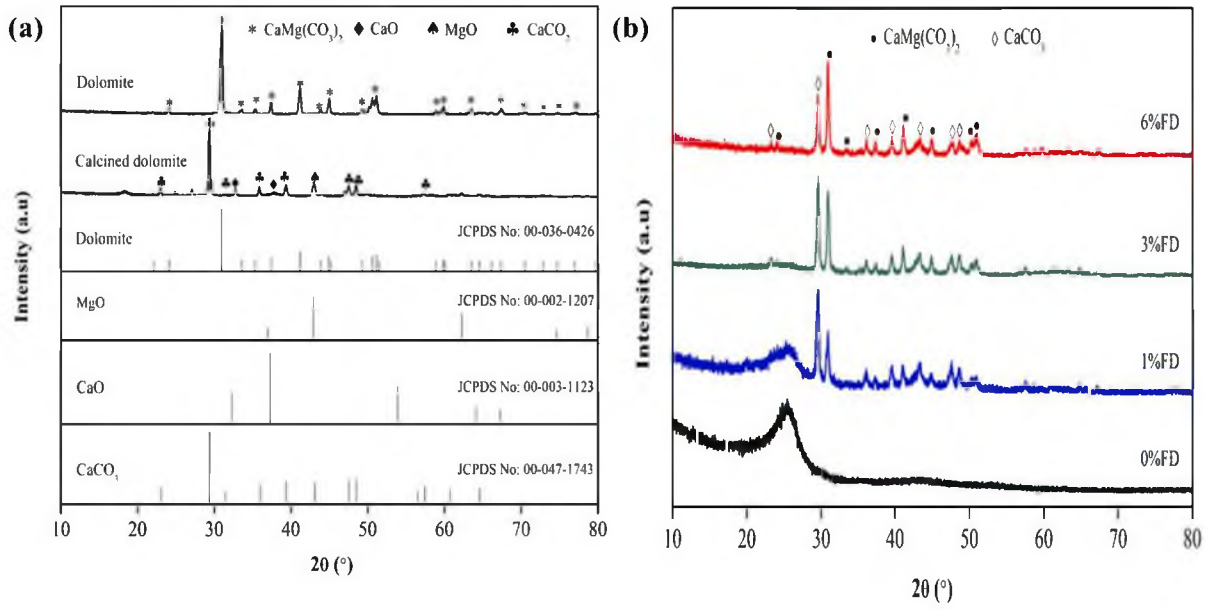

Fig. 3. XRD analysis of (a) dolomite and calcined dolomite and (b) spent catalysts recovered from pyrolysis of WCO at different dolomite loading.

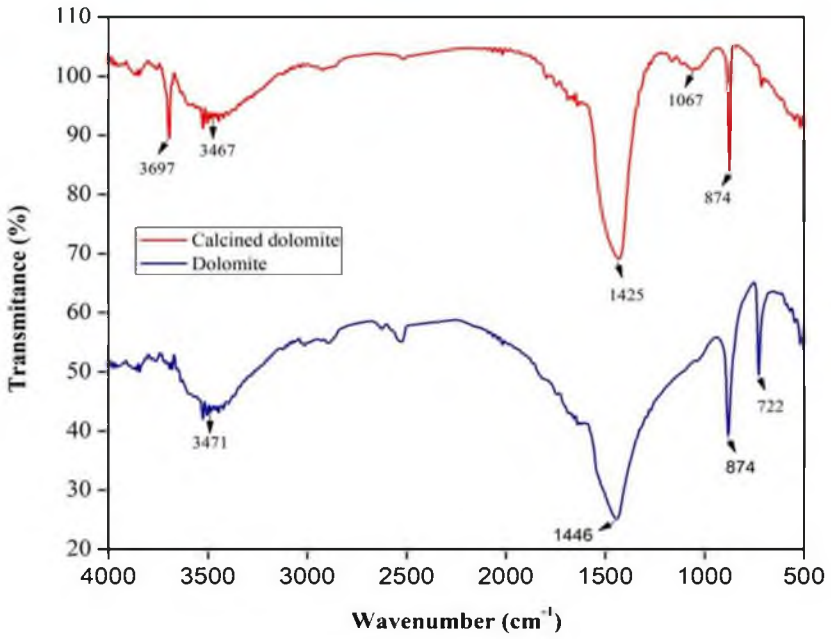

Fig. 4. FTIR analysis of dolomite and calcined dolomite.

3697 cm^{-1}. However, the peak at 722 cm^{-1} as the main characteristic of dolomite disappeared in calcined dolomite, which indicates the transformation of dolomite into CaO and MgO. The formation of new peaks at 1067 cm^{-1} is ascribed to the asymmetric stretching of carbonate (Wang, 2019), and 3697 cm^{-1} as the OH stretching vibration of $Ca(OH)_2$ formed by the hydration of CaO (Carretti et al., 2013).

The N_2 adsorption-desorption isotherm and pore size distribution of dolomite and calcined dolomite were presented in Fig. 5. Both dolomite and calcined dolomite were identified as type II isotherms of non-porous material. Calcined dolomite showed a low hysteresis loop at P/P0 = 0.9–1.0 with increased N_2 uptake. At higher P/P_0, hysteresis for capillary condensation is caused by the presence of mesopores between CaO-MgO particles. In calcined dolomite, high temperatures accelerate the thermal decomposition of dolomite which can modify the chemical and physical structure that might affect the catalytic reaction. Table 2 summarized the textural properties of dolomite and calcined dolomite. Dolomite without calcination has a low surface area and pore volume compared to calcined dolomite. The surface area of dolomite is 3.984 m^2g^{-1} and calcined dolomite is 9.708 m^2g^{-1}.

Fig. 6 shows the SEM-EDX analysis of dolomite and calcined dolomite. Calcined dolomite has an irregular cube-like crystal structure with non-uniform sizes. However, calcined dolomite formed cube-like

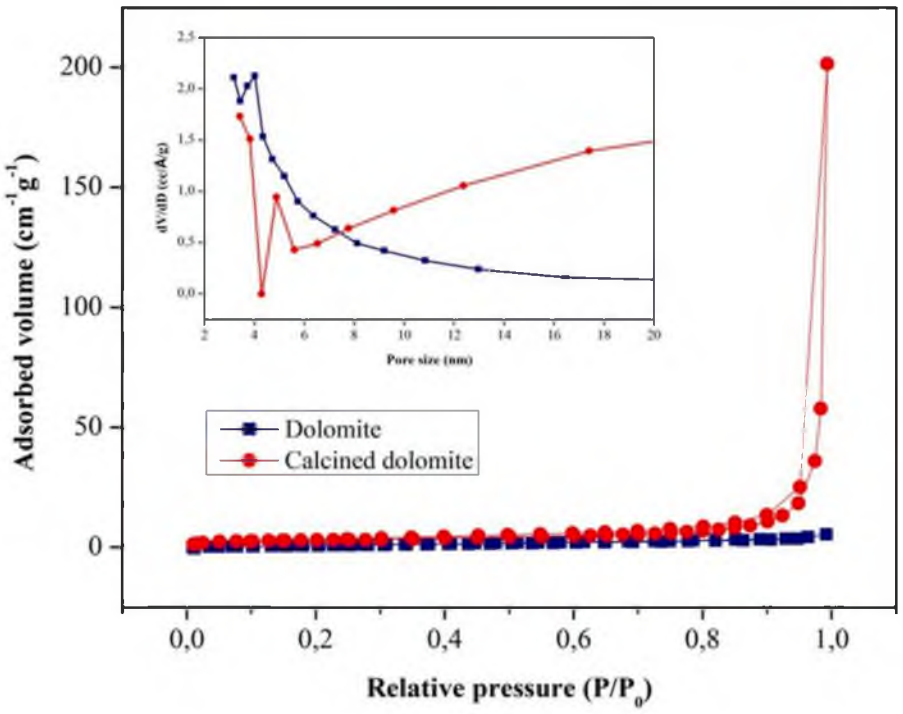

Fig. 5. N_2 adsorption-desorption isotherm and pore size distribution of dolomite and calcined dolomite.

Table 2
Physicochemical properties of dolomite and calcined dolomite.

Sample	Surface area (m^2g^{-1}) [a]	Volume (cm^3g^{-1}) [b]	Pore size (nm)[b]	Phase content [c]	Phase composition (wt.%) [d]	Wt.% elemental composition [e]			
						Ca	C	O	Mg
Dolomite	3.984	0.0078	4.01	Dolomite	100	45	7	28	20
Calcined dolomite	9.708	0.31	4.87	CaO	14.93	41	–	39	20
				MgO	10.06				
				$CaCO_3$	75.01				

[a] S_{BET} (surface area) by BET method.
[b] BJH calculated by N_2 desorption.
[c] XRD analysis.
[d] Calculated using Rietica software.
[e] EDX analysis.

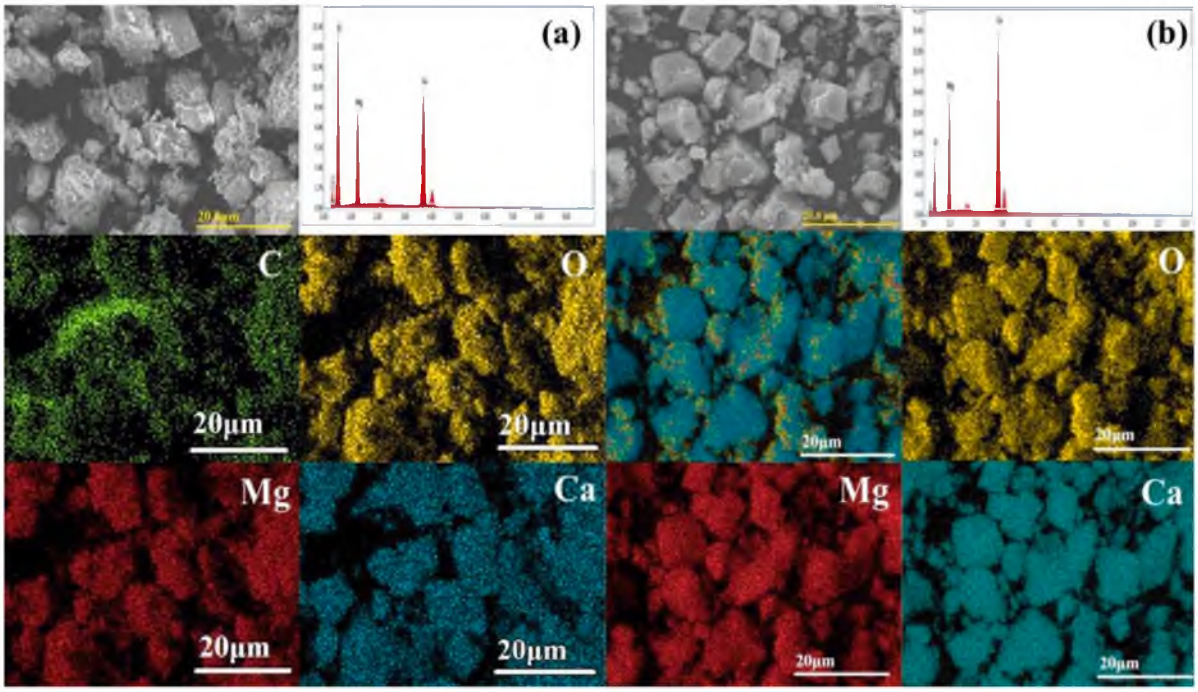

Fig. 6. SEM-EDX analysis of (a) dolomite and (b) calcined dolomite.

crystals with flat surfaces. The non-uniform small aggregates disappeared from calcined dolomite. Table 2 summarized the elemental composition of dolomite and calcined dolomite obtained from EDX analysis. Dolomite has constituent elements of C: 7 wt%; Ca: 45 wt%; O: 28 wt% and Mg: 20 wt%. Following calcination at 850 °C, carbon disappeared, thus changing the composition to Ca: 41 wt%, O: 39 wt%, and Mg: 20 wt%.

3.3. *Thermal and catalytic pyrolysis of WCO*

Pyrolysis of WCO was conducted in the absence of catalysts referred to as thermal pyrolysis, and catalytic pyrolysis using calcined dolomite and fresh dolomite. Pyrolysis parameters have significant effects on product distribution and liquid bio-oil composition. In this work, the effects of temperature, the amount of dolomite loading, and the pyrolysis time were examined on the composition of the liquid bio-oil product.

3.3.1. *Effect of temperature on thermal pyrolysis*

The effect of temperature was conducted on thermal pyrolysis with the absence of catalysts at 350, 450, and 550 °C. The temperature at 350 °C was chosen based on the TGA analysis of WCO that indicated the fatty acid decomposition begins at 320 °C. Fig. 7 shows the bio-oil yield

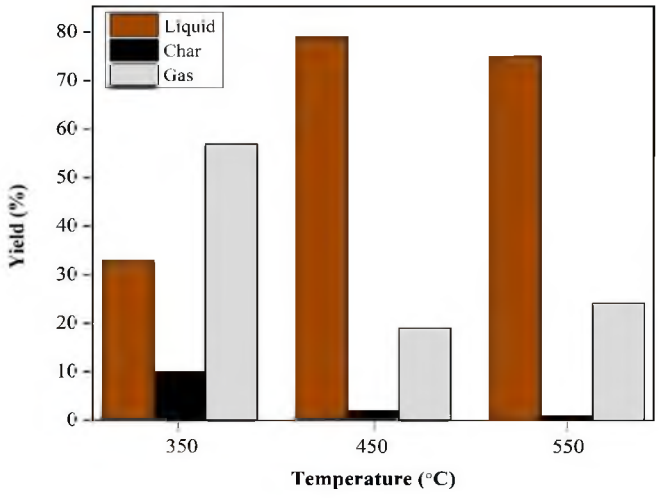

Fig. 7. Product yield of non-catalytic themal pyrolysis of WCO at different temperatures.

increased from 33% at 350 °C to 79% at 450 °C, with a significant reduction of non-condensable gas from 57% to 19%. At 450 °C, the decomposition of heavy molecules in the feedstock increased the liquid yield production. Pyrolysis at high temperatures provides sufficient thermal energy to dissociate the strong organic bonds in fatty acids. When the pyrolysis was conducted at 550 °C, the bio-oil yield was slightly decreased to 75%. The bio-char product also decreased at 550 °C to give only 0.9%, but the non-condensed gas yield increased from 19% to 24.1%. High temperatures promoted the secondary cracking reaction which decreased the formation of bio-char but yielded non-condensable gas. The bio-char was produced from the polymerization of aromatic hydrocarbons and direct condensation reaction of WCO (Hafriz et al., 2021). The high pyrolysis temperatures accelerated the kinetics of fatty acids decomposition through a secondary cracking reaction. Rapid endothermic decomposition of WCO caused the condensable gas to be further converted to the non-condensable gas (Dai et al., 2019; Bartoli et al., 2016). Therefore, high temperatures caused the formation of gasses as the dominant products, and hence reduced the liquid yield production (Williams and Nugranad, 2000; He et al., 2018; Zhang et al., 2015).

3.3.2. *Catalytic pyrolysis*

Since the optimum temperature for pyrolysis of WCO into liquid yield was obtained at 450 °C, all the catalytic pyrolysis using fresh dolomite, calcined dolomite, optimization of dolomite loading, and reaction time were conducted at 450 °C. Fig. 8 shows the product distribution and the time required to achieve 100% WCO conversion, when pyrolysis was conducted without dolomite (0%FD), using 1%, 3% and 6% of fresh dolomite (FD), and when using 6% calcined dolomite (CD). Liquid bio-oil yield was slightly decreased from 73.46% when using 1% of fresh dolomite (1%FD) to 68.37% as the amount of fresh dolomite increased to 6% (6%FD). The gas product was enhanced from 24.71% to 30.99% with the increase in dolomite concentration. The presence of high catalyst loading was suggested to lengthen the reactant residence time and initiate the subsequent thermal cracking into low molecular weights gasses (Pütün, 2010; Mishra and Mohanty, 2018). The production of char dropped from 1.82 at 0%FD to 0.64% as the catalyst loading increased to 6%FD (Fig. 8). Increasing the loading of dolomite catalysts enhanced the breaking of the carbon chain to form lower carbon molecules and non-condensable gas (Wang et al., 2019). Furthermore, the formation of dolomite/$CaCO_3$ phases (Fig 3b) may have a significant role in reducing char formation as reported on K_2CO_3 promoter, in which the carbonate enhanced the gasification of carbon char into gas products in the steam reforming of biomass-derived tar (Kuchonthara et al., 2012).

The use of fresh dolomite in pyrolysis significantly reduced the time required for complete WCO conversion into products. Controlling the reaction time is crucial in achieving a high yield of liquid bio-oil hydrocarbon by preventing secondary reactions such as carbonization, gasification and thermal cracking, which reduced bio-oil production (Bartoli et al., 2016; Tsai et al., 2007). Fig. 8 shows that in the absence of dolomite (0%FD), the pyrolysis takes place within 141 min to completely decompose the WCO. The reaction time to achieve 100% WCO conversion was reduced when using a higher dolomite loading, requiring only 75 min at 6%FD. The pyrolysis time was reduced by 50% to complete the pyrolysis reaction compared to the 140 min required in the absence of dolomite.

Catalytic pyrolysis was also conducted using calcined dolomite in the form of CaO/MgO mixture at 6% (6%CD). The liquid yield was slightly reduced to 61.12%, while the bio-char and uncondensed gas increased to 6.36% and 32.52%, respectively. The pyrolysis required 98 min to complete when using calcined dolomite as the catalyst. The amount of liquid yield is lower than when using fresh dolomite and without catalyst, although the value is higher than the reported studies on CaO/MgO catalyst at 21.23 wt.% and 47.8 wt.% (Valle et al., 2014; Shahruzzaman et al., 2018). In dolomite, stable basic sites allowed the pyrolysis of fatty acids in WCO into liquid product. However, calcination of dolomite formed CaO/MgO mixtures that changes the active sites and the basicity of catalyst. MgO reduced the acid composition of bio-oil through ketonization and condensation aldol (Valle et al., 2019), while CaO catalyzed the decarboxylation reaction to form hydrocarbon (Chen et al., 2019). The deoxygenation of hydroxyl, carbonyl and carboxyl compounds occurred on CaO, which leads to the formation of aliphatic hydrocarbons (Wu et al., 2022). MgO was reported to catalyze the

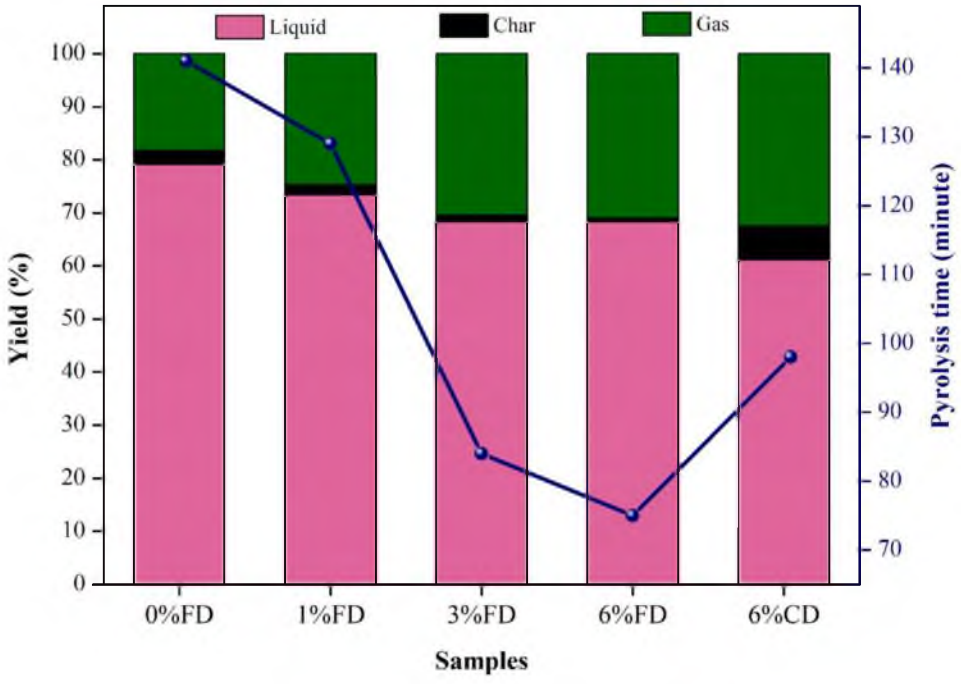

Fig. 8. The bio-oil yield and the determined pyrolysis time at 450 °C from thermal pyrolysis (0%FD) and catalytic pyrolysis using dolomite (FD 1%, 3%, and 6%) and 6% calcined dolomite.

decomposition of volatile macromolecular compounds and prevent the deactivation of CaO active sites caused by char formation (Islam, 2020). Charusiri, 2017 reported that CaO and MgO were very effective in removing carboxyl and carbonyl groups from bio-oil (Charusiri and Vitidsant, 2017). However, the synergy between CaO and MgO reduced the formation of carbon from aliphatic hydrocarbons and produced more volatiles into non-condensable gasses (Pütün, 2010). The basicity of CaO/MgO also tends to capture CO_2 which leads to the formation of $CaCO_3$ and bio-char (Valle et al., 2020).

Fig. 9a shows the distribution of chemical composition in liquid yield analyzed using GCMS. Although 0%FD produced a high amount of liquid product, the liquid yield predominantly contained carboxylic acids at 85.7 wt.%, followed by hydrocarbons at 12.81 wt.%, and ketones at 1.49 wt.%. The hydrocarbon composition increases when using a higher dolomite loading, to give 56.23 wt.% of hydrocarbon yield at 6%FD. Since the amount of carboxylic acid decreased with the increasing dolomite concentration, the result indicates the role of dolomite as the catalyst for removing the oxygenated fragment in the fatty acids. The basic sites on dolomite adsorbed fatty acid molecules through carbon carbonyl to initiate C—O bond dissociation, removing the -COOH fragment.

Fig. 9b shows the composition of saturated and unsaturated hydrocarbon in the liquid yield. The pyrolytic oil produced in the absence of dolomite mainly contained alkane at 90.11% selectivity. The use of 1% dolomite produced an approximately equal ratio of alkene and alkane, while 6% FD 64.44% alkane selectivity. Bio-oil riches with aliphatic hydrocarbon composition have the potential to be developed as a fuel source. Fig. 9c illustrates the effect of catalyst loading on hydrocarbon distribution. Heavy oil is the dominant product from thermal pyrolysis (0%FC) compared to diesel hydrocarbon from catalytic pyrolysis. The amount of catalyst loading directly correlates with the production of the gasoline and diesel fractions. The bio-oil obtained from the pyrolysis of WCO can be upgraded to produce transport grade diesel based on the analysis of the physical properties of biofuel in Table 3.

3.3.3. *Effect of pyrolysis time*

Monitoring the composition of liquid bio-oil obtained from catalytic pyrolysis of WCO at different reaction times provides insight into the mechanism of reaction. A total of 1500 g of WCO feedstock and 6% dolomite were added into the reactor, and the liquid products were collected at different times up to 75 min. The pyrolysis time was counted starting from the first release of bio-oil into the collection outlets. Fig. 10 shows the transformation of WCO into liquid and gas products occurred at a similar rate 15 min into the reaction before liquid bio-oil gradually dominated the products at 75 min. The uncondensed gas yield reached 28% within 15 min of the reaction, with only a slight increase within 75 min to give 30% selectivity. Bio-char begins to form after 75 mins. Under a controlled reaction time, the secondary reaction involving the conversion of triglycerides into lighter hydrocarbons can be suppressed which evetually might lead to carbon char formation (Muhammad et al., 2021).

Analysis of the liquid bio-oil indicates the conversion of WCO into hydrocarbon was increased from 38.99% to 57.27% as pyrolysis time increased to 75 min (Fig. 10a). Carboxylic acid dominates the bio-oil composition at the early pyrolysis process, suggesting the WCO decomposed via a cracking reaction to form short chain carboxylic acid (Fig. 11a). Longer pyrolysis times are important to decrease the amount of acid in the liquid oil product, by allowing the decarboxylation/-

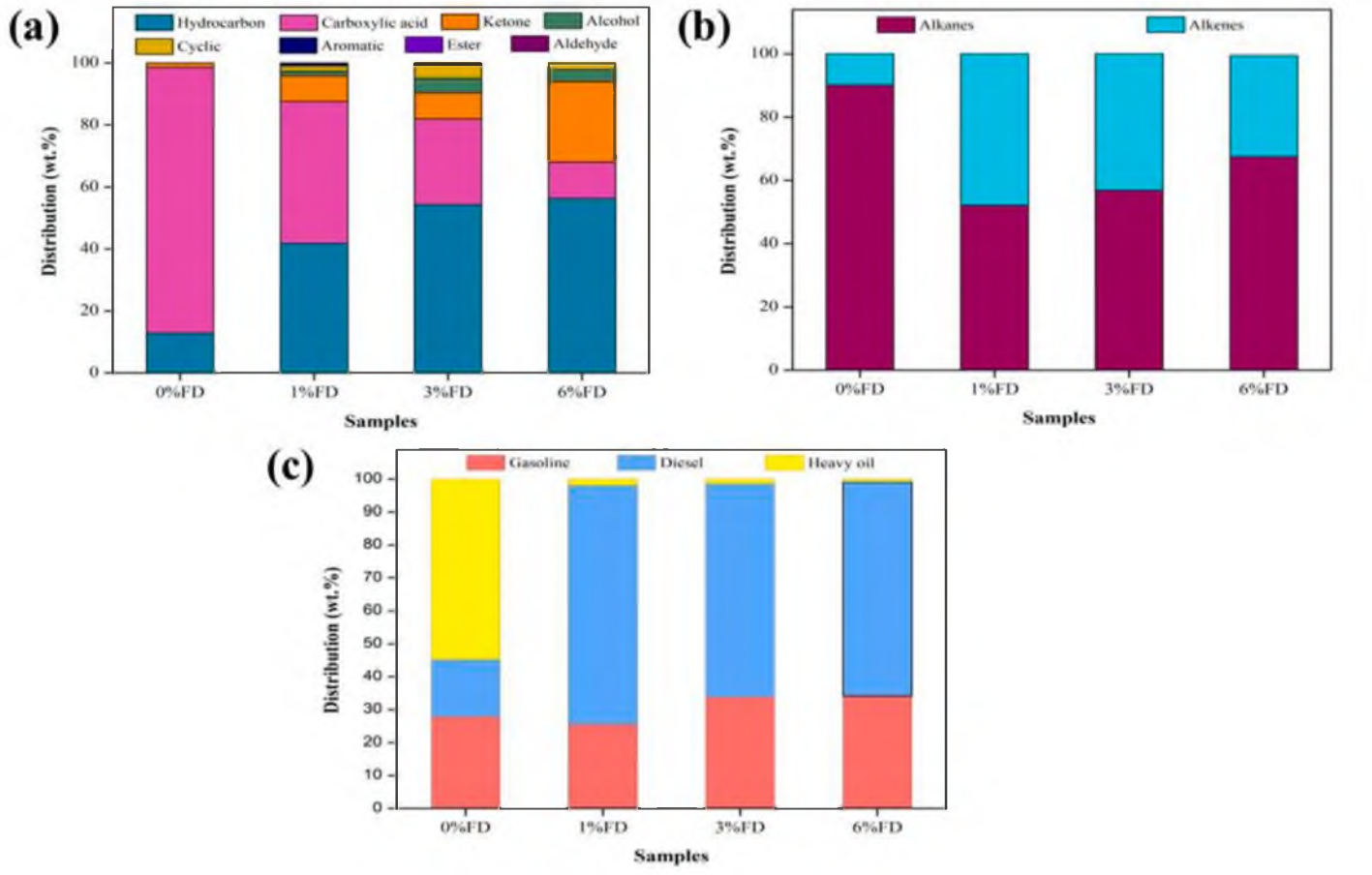

Fig. 9. The distribution of liquid product yield composition based on (a) functional group; (b) alkene/alkane aliphatic hydrocarbon; (c) hydrocarbon range in gasoline, diesel and heavy oil. Reaction was conducted at 450 °C.

Table 3
The physical properties of biofuel.

Properties	Thermal pyrolysis of WCO	Catalytic pyrolysis of WCO (loading catalyst)			Gasoline (EN228)	Diesel fuel (EN590)
		1%	3%	6%		
Viscosity (cSt)	3.19	4.35	2.34	2.51	–	2.0–4.5
Density (gcm^{-3})	0.85	0.86	0.83	0.84	0.72–0.77	0.82–0.84
Calorific value (MJ/kg)	39.86	40.45	41.79	42.05	42.41–46.51	42.7

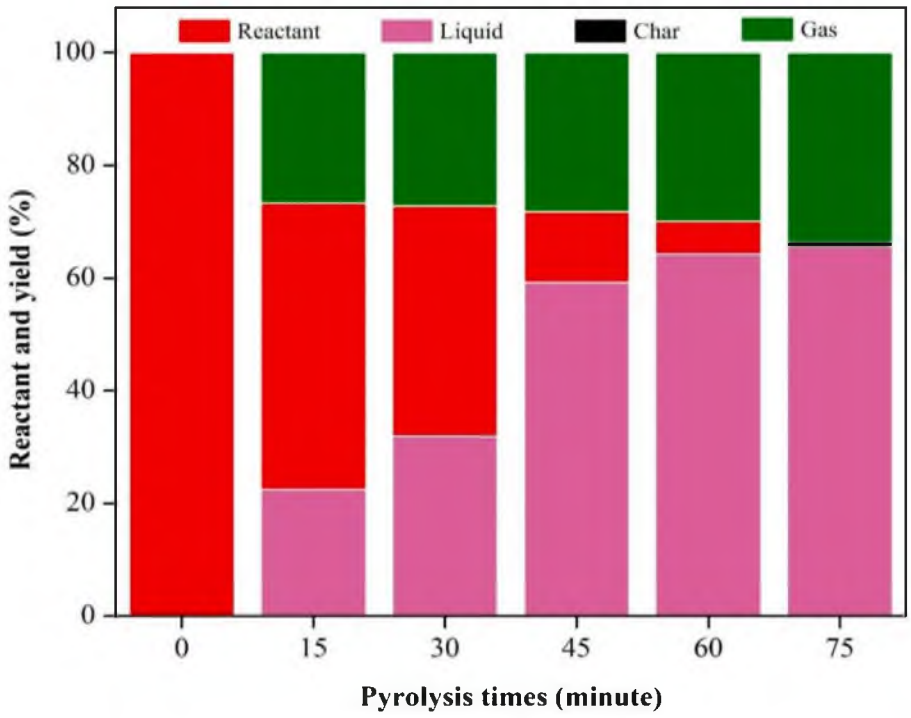

Fig. 10. Distribution of WCO reactant and product composition obtained using 6% dolomite catalyst at different pyrolysis times.

decarbonylation reaction of fatty acids into hydrocarbon (Wan Mahari et al., 2021).

The selectivity of alkanes and alkenes was relatively similar with increasing the pyrolysis time, although alkanes are the dominant hydrocarbon (Fig. 11b). The liquid bio-oils are further divided into three fractions, namely gasoline (C_{6-12}), diesel (C_{13-20}), and heavy oil ($>C_{20}$) (Syamsiro et al., 2014). Fig. 11c shows the heavy oil fraction reduced while the gasoline hydrocarbon enhanced with increasing pyrolysis time. The results indicate that extending the pyrolysis time efficiently transforms carboxylic acid into hydrocarbon via deoxygenation, then followed by catalytic cracking into short-chain hydrocarbon. Hydrocarbons in diesel composition were identified as the main product, with no significant changes in selectivity throughout the reaction.

Analysis of products obtained from thermal pyrolysis and catalytic pyrolysis of WCO showed the role of dolomite to accelerate the pyrolysis process while simultaneously increasing the formation of hydrocarbon fuel. XRD of the spent dolomite recovered after pyrolysis of WCO is shown in Fig. 12. Dolomite was transformed to calcium carbonate within 15 min of the reaction, and the intensity of XRD $CaCO_3$ peaks was enhanced at longer pyrolysis time. However, the peaks corresponding to dolomite were still observed up to 75 min suggesting dolomite transformed into dolomite/$CaCO_3$ phases via partial separation as will be described in the following section.

3.4. Catalyst reusability and stability test

Analysis of dolomite recovered after pyrolysis indicated the formation of dolomite and calcium carbonate. Therefore, a reusability study was conducted to determine the stability of the dolomite catalyst under optimal pyrolysis reaction conditions. The recovered catalyst was washed with n-hexane until the color of the filtration was clear to remove char. The catalyst was reused without any further treatment for another two reaction cycles. Fig. 13 shows only slight changes on the liquid yield, uncondensed gas and char production. The liquid bio-oil products were determined at 68.37%, 60.08%, and 62.26%, respectively (Su et al., 2022), while carbon char was slightly increased from 0.64 to 1.86%. Dolomite still maintained a high productivity that indicated its reusability and stability as a catalyst despite a clear transformation of dolomite to calcium carbonate. The XRD analysis of the spent catalysts showed the formation of biochar deposited on the catalyst together with the dolomite and $CaCO_3$ peaks (Fig 14a). The results were supported by the FTIR results in Fig. 14a indicating the increased intensity of 2851 and 2923 cm^{-1} bands as the typical hydrocarbon molecules of carbon char deposition (Wang et al., 2019).

Generally, calcium carbonate is produced at 700 °C when dolomite is annealed at high temperatures (Conesa and Domene, 2015; Charusiri and Vitidsant, 2017; Correia et al., 2015). However, XRD analysis on the recovered catalysts showed a mixture of dolomite and calcite ($CaCO_3$) was formed within 15 min of pyrolysis although the pyrolysis reaction was conducted at 450 °C. The results indicate structural rearrangement of dolomite has occurred during pyrolysis of WCO. Dolomite can undergo partial separation into magnesite-calcite solid solution or primary separation into the two carbonates under CO_2 atmosphere. The presence of carbon dioxide controls the kinetic decomposition of dolomite (E.S.P. B. et al., 1990; Caceres and Attiogbe, 1997). In CO_2 atmosphere, dolomite decomposition occurs at low temperatures than under air or

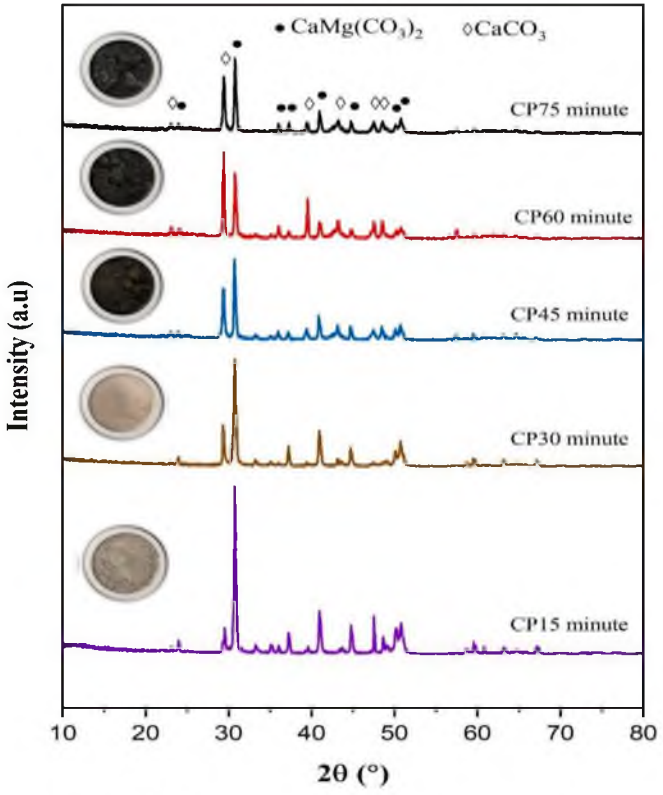

Fig. 12. XRD analysis of spent catalyst at different pyrolysis times.

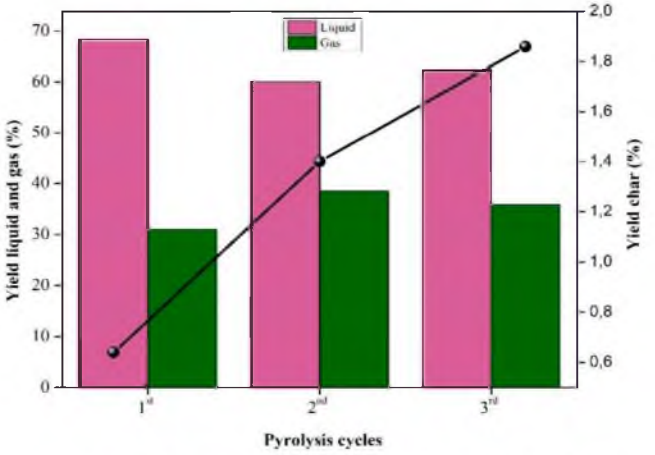

Fig. 13. Reusability of dolomite catalysts in the pyrolysis of WCO.

nitrogen environment (Hashimoto and Uematsu, 1980). Although no CO_2 flow was introduced during pyrolysis, the continuous generation CO_2 during the thermal decomposition of WCO creates CO_2 rich environment that initiates the separation of dolomite.

Partial Separation:

$$MgCa(CO_3)_2 \rightarrow CaCO_3.MgCO_3 \quad (7)$$

Primary separation:

$$MgCa(CO_3)_2 \rightarrow CaCO_3 + MgCO_3 \quad (8)$$

In primary separation, magnesite is formed in a metastable state that

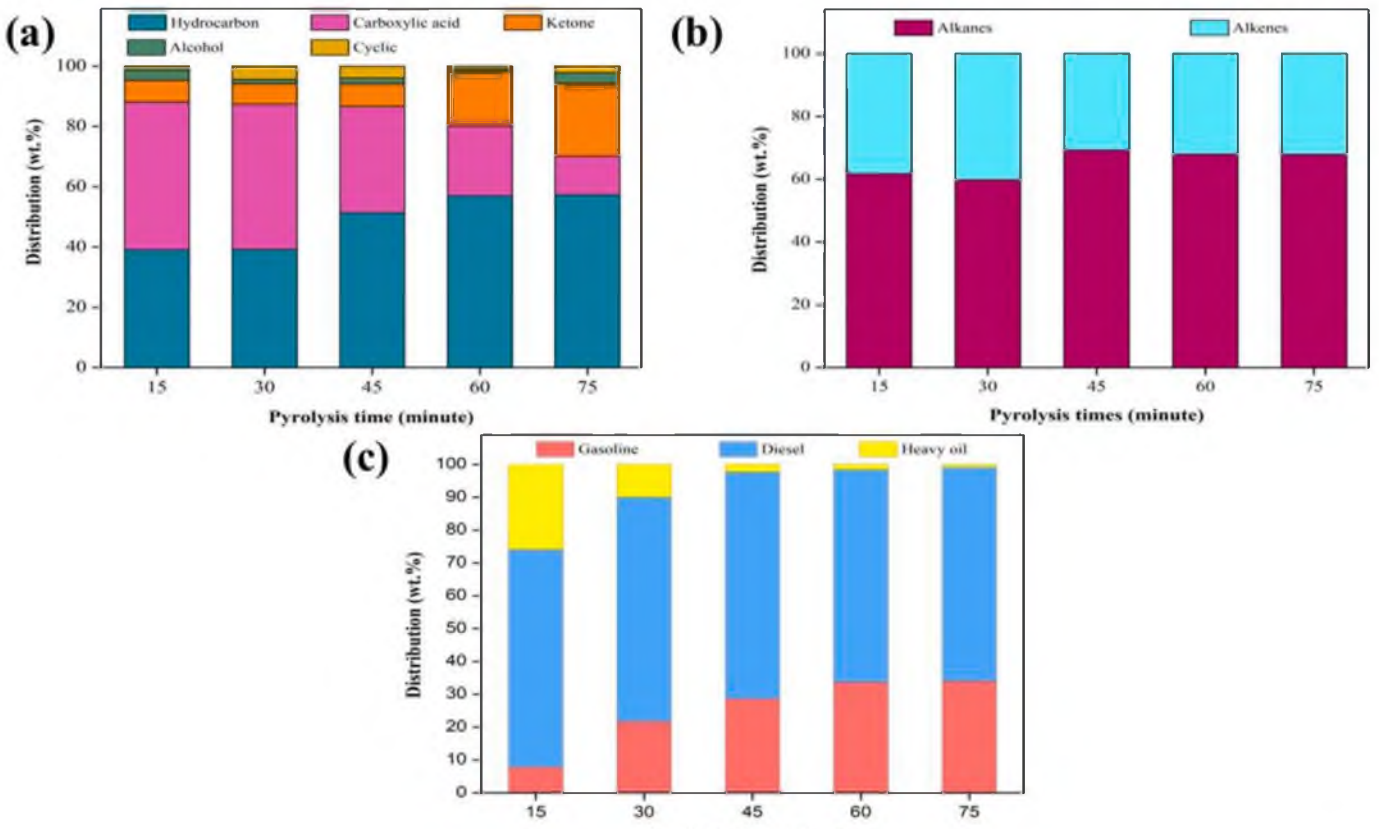

Fig. 11. The distribution of liquid product yield composition based on (a) functional group; (b) alkene/alkane aliphatic hydrocarbon; (c) hydrocarbon range in gasoline, diesel and heavy oil. Reaction was conducted at 450 °C while using 6% dolomite at different pyrolysis time.

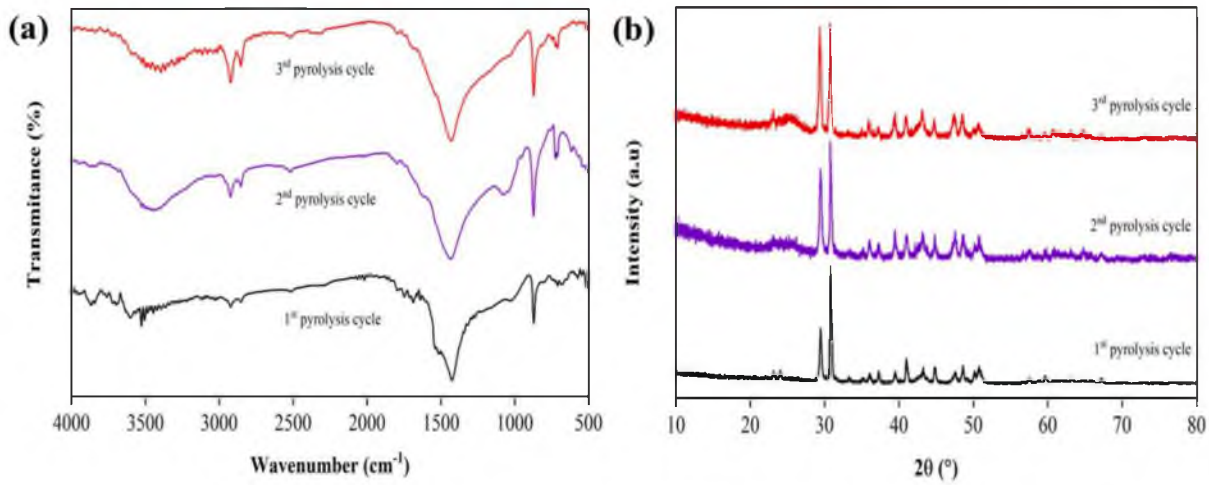

Fig. 14. FTIR (a) and XRD analysis (b) of the spent catalyst recovered at different pyrolysis cycles.

subsequently decomposes into MgO. However, XRD of the recovered catalyst only showed the formation of calcite ($CaCO_3$), with no significant peaks assigned to $MgCO_3$ or MgO. There is a possibility that due to lower Mg concentration (20%) than Ca (40%) in dolomite, the XRD peaks of $MgCO_3$ are indistinguishable by XRD. Calcite formation may follow direct separation from dolomite or re-carbonation by reaction with carbon dioxide generated during pyrolysis of WCO. This provides an interesting aspect of the dolomite ability to catalyze WCO pyrolysis into diesel hydrocarbon while simultaneously acting as an adsorbent to reduce CO_2 emission to the atmosphere. If dolomite undergoes decomposition into its corresponding oxides, a high level of CO_2 was released, consequently disrupting the crystal structure of dolomite. Since no significant changes on the XRD peaks of dolomite, it suggested that calcite is formed via counter-migration of Ca^{2+} and Mg^{2+} ions (E.S.P.B. et al., 1990) from the dolomite, preserving the crystal structure of dolomite (Fig. 14b).

4. Conclusion

Pyrolysis of WCO into liquid bio-oil was successfully conducted using dolomite as the catalyst. In thermal pyrolysis, the optimum temperature was determined at 450 °C, which produced the maximum yield of bio-oil at 79%. However, the liquid bio-oil from thermal pyrolysis contained a high percentage of carboxylic acids. Dolomite is crucial to enhance the hydrocarbon yield via deoxygenation of carboxylic acid and reducing the pyrolysis time from 141 min to 75 min. The deoxygenation reaction during catalytic pyrolysis increased the production of diesel and gasoline hydrocarbons. Dolomite shows phase separation to form dolomite/$CaCO_3$ mixtures that occurred during the initial stage of the pyrolysis process. The stability of dolomite for three reaction cycles indicated the synergy of dolomite/$CaCO_3$ to achieve high selectivity to hydrocarbon while reducing the formation of biochar.

Declaration of competing interest

The authors declare that they have no known competing financial interests or personal relationships that could have appeared to influence the work reported in this paper.

Acknowledgements

Support from Ministry of Education, Culture, Research, and Technology under PDD research grant with contract number 833/PKS/ITS/2021 and ITS project scheme of the Publication Writing and IPR Incentive Program (PPHKI) 2023 are gratefully acknowledged.

References

Bartoli, M., Rosi, L., Giovannelli, A., Frediani, P., Frediani, M., 2016. Production of bio-oils and bio-char from Arundo donax through microwave assisted pyrolysis in a multimode batch reactor. J. Anal. Appl. Pyrolysis. 122, 479–489. https://doi.org/10.1016/J.JAAP.2016.10.016.

Ben Hassen Trabelsi, A., Zaafouri, K., Baghdadi, W., Naoui, S., Ouerghi, A., 2018. Second generation biofuels production from waste cooking oil via pyrolysis process. Renew. Energy. 126, 888–896. https://doi.org/10.1016/J.RENENE.2018.04.002.

Berrueco, C., Montané, D., Matas Güell, B., del Alamo, G., 2014. Effect of temperature and dolomite on tar formation during gasification of torrefied biomass in a pressurized fluidized bed. Energy 66, 849–859. https://doi.org/10.1016/J.ENERGY.2013.12.035.

Caceres P.G., Attiogbe E.K., Thermal decomposition of dolomite a n d the extraction of its constituents, 10 (1997) 1165–1176.

Carretti E., Chelazzi D., Rocchigiani G., Baglioni P., Poggi G., Dei L., Interactions between Nanostructured Calcium Hydroxide and Acrylate Copolymers: implications in Cultural Heritage Conservation, (2013).

Charusiri, W., Vitidsant, T., 2017. Upgrading bio-oil produced from the catalytic pyrolysis of sugarcane (Saccharum officinarum L) straw using calcined dolomite. Sustain. Chem. Pharm. 6, 114–123. https://doi.org/10.1016/J.SCP.2017.10.005.

Chen T., Li H., Wang H., Removal of Pb (II) from Aqueous Solutions by Periclase /Calcite Nanocomposites, (2019).

Chen, X., Chen, Y., Yang, H., Wang, X., Che, Q., Chen, W., Chen, H., 2019b. Catalytic fast pyrolysis of biomass: selective deoxygenation to balance the quality and yield of bio-oil. Bioresour. Technol. 273, 153–158.

Conesa, J.A., Domene, A., 2015. Gasification and pyrolysis of Posidonia oceanica in the presence of dolomite. J. Anal. Appl. Pyrolysis. 113, 680–689. https://doi.org/10.1016/J.JAAP.2015.04.019.

Correia, L.M., de Sousa Campelo, N., Novaes, D.S., Cavalcante, C.L., Cecilia, J.A., Rodríguez-Castellón, E., Vieira, R.S., 2015. Characterization and application of dolomite as catalytic precursor for canola and sunflower oils for biodiesel production. Chem. Eng. J. 269, 35–43. https://doi.org/10.1016/J.CEJ.2015.01.097.

Dai, L., Wang, Y., Liu, Y., Ruan, R., Yu, Z., Jiang, L., 2019. Science of the Total Environment Comparative study on characteristics of the bio-oil from microwave-assisted pyrolysis of lignocellulose and triacylglycerol. Sci. Total Environ. 659, 95–100. https://doi.org/10.1016/j.scitotenv.2018.12.241.

E.S.P.B. V., R.M. Mcintosh, J.H. Sharp, F.W. Wilburn, The thermal decomposition of dolomite, 165 (1990) 281–296.

G. Fadillah, I. Fatimah, I. Sahroni, M.M. Musawwa, Recent Progress in Low-Cost Catalysts for Pyrolysis of Plastic, (2021).

Galadima, A., Muraza, O., 2015. Catalytic upgrading of vegetable oils into jet fuels range hydrocarbons using heterogeneous catalysts: a review. J. Ind. Eng. Chem. 29, 12–23. https://doi.org/10.1016/j.jiec.2015.03.030.

Gao, J., Zhang, Y., Meng, D., Jiao, T., Qin, X., Bai, G., Liang, P., 2019. Effect of ash and dolomite on the migration of sulfur from coal pyrolysis volatiles. J. Anal. Appl. Pyrolysis. 140, 349–354. https://doi.org/10.1016/J.JAAP.2019.04.013.

Ge, S., Ganesan, R., Sekar, M., Xia, C., Shanmugam, S., Alsehli, M., Brindhadevi, K., 2022. Blending and emission characteristics of biogasoline produced using CaO /SBA-15 catalyst by cracking used cooking oil. Fuel 307, 121861. https://doi.org/10.1016/j.fuel.2021.121861.

Gielen, D., Boshell, F., Saygin, D., Bazilian, M.D., Wagner, N., Gorini, R., 2019. The role of renewable energy in the global energy transformation. Energy Strateg. Rev. 24, 38–50. https://doi.org/10.1016/j.esr.2019.01.006.

Guo, X., Xia, A., Li, F., Huang, Y., Zhu, X., Zhang, W., Zhu, X., Liao, Q., 2022. Photoenzymatic decarboxylation to produce renewable hydrocarbon fuels: a comparison between whole-cell and broken-cell biocatalysts. Energy Convers. Manag. 255, 115311 https://doi.org/10.1016/j.enconman.2022.115311.

Hafriz, R.S.R.M., Shafizah, I.N., Arifin, N.A., Salmiaton, A., Yunus, R., Yap, Y.H.T., Shamsuddin, A.H., 2021. Effect of Ni/Malaysian dolomite catalyst synthesis technique on deoxygenation reaction activity of waste cooking oil. Renew. Energy. 178, 128–143. https://doi.org/10.1016/j.renene.2021.06.074.

Hashimoto H., Uematsu T., Partial Decomposition of Dolomite in CO, (1980) 181–188.

Hatefirad, P., Tavasoli, A., 2021. Effect of acid treatment and Na2CO3 as a catalyst on the quality and quantity of bio-products derived from the pyrolysis of granular bacteria biomass. Fuel 295, 120585. https://doi.org/10.1016/J.FUEL.2021.120585.

He, X., Liu, Z., Niu, W., Yang, L., Zhou, T., Qin, D., Niu, Z., Yuan, Q., 2018. Effects of pyrolysis temperature on the physicochemical properties of gas and biochar obtained from pyrolysis of crop residues. Energy 143, 746–756. https://doi.org/10.1016/j.energy.2017.11.062.

Ibarra, Á., Hita, I., Azkoiti, M.J., Arandes, J.M., Bilbao, J., 2019. Journal of Industrial and Engineering Chemistry Catalytic cracking of raw bio-oil under FCC unit conditions over different zeolite-based catalysts. J. Ind. Eng. Chem. 78, 372–382. https://doi.org/10.1016/j.jiec.2019.05.032.

Islam, M.W., 2020. A review of dolomite catalyst for biomass gasification tar removal. Fuel 267, 117095. https://doi.org/10.1016/J.FUEL.2020.117095.

Jeswani, H.K., Chilvers, A., Azapagic, A., 2020. Environmental sustainability of biofuels: a review: environmental sustainability of biofuels. Proc. R. Soc. A Math. Phys. Eng. Sci. 476 https://doi.org/10.1098/rspa.2020.0351.

Ji, J., Ge, Y., Balsam, W., Damuth, J.E., Chen, J., 2009. Rapid identification of dolomite using a Fourier Transform Infrared Spectrophotometer (FTIR): a fast method for identifying Heinrich events in IODP Site U1308. Mar. Geol. 258, 60–68. https://doi.org/10.1016/J.MARGEO.2008.11.007.

Kanchanatip, E., Chansiriwat, W., Palalerd, S., 2022. Light biofuel production from waste cooking oil via pyrolytic catalysis cracking over modified Thai dolomite catalysts. Carbon Resour. Convers. 5, 177–184. https://doi.org/10.1016/j.crcon.2022.05.001.

Kang, Y., Wei, X., Zhang, X., Li, Y., 2021. Deep catalytic hydroconversion of straw-derived bio-oil to alkanes over mesoporous zeolite Y supported nickel nanoparticles. Renew. Energy. 173, 876–885. https://doi.org/10.1016/j.renene.2021.04.003.

Kassa, T., Islam, A., Kumar, R., Scott, J., Antunes, E., 2022. Catalytic co-pyrolysis of ironbark and waste cooking oil using strontium oxide-modified Y-zeolite for high-quality bio-oil production. Chem. Eng. J. 450, 138448 https://doi.org/10.1016/j.cej.2022.138448.

Kuchonthara P., Puttasawat B., Piumsomboon P., Mekasut L., Vitidsant T., Catalytic steam reforming of biomass-derived tar for hydrogen production with K 2 CO 3 /NiO / γ -Al 2 O 3 catalyst, 29 (2012) 1525–1530. https://doi.org/10.1007/s11814-012-0027-y.

Li, H., Wang, Y., Zhou, N., Dai, L., Deng, W., Liu, C., Cheng, Y., Liu, Y., Cobb, K., Chen, P., Ruan, R., 2021. Applications of calcium oxide e based catalysts in biomass pyrolysis /gasi fi cation e A review. J. Clean. Prod. 291, 125826 https://doi.org/10.1016/j.jclepro.2021.125826.

Long, F., Zhai, Q., Liu, P., Cao, X., Jiang, X., Wang, F., Wei, L., Liu, C., Jiang, J., Xu, J., 2020. Catalytic conversion of triglycerides by metal-based catalysts and subsequent modification of molecular structure by ZSM-5 and Raney Ni for the production of high-value biofuel. Renew. Energy. 157, 1072–1080. https://doi.org/10.1016/J.RENENE.2020.05.117.

Luo, Y., Zhu, L., He, Y., Yang, M., Zhang, Y., 2022. Selective catalytic transformation of cellulose into bio-based cresol with CuCr 2 O 4 @ MCM-41 catalyst. Cellulose 29, 303–319. https://doi.org/10.1007/s10570-021-04285-9.

Ly, H.V., Lim, D.H., Sim, J.W., Kim, S.S., Kim, J., 2018. Catalytic pyrolysis of tulip tree (Liriodendron) in bubbling fluidized-bed reactor for upgrading bio-oil using dolomite catalyst. Energy 162, 564–575. https://doi.org/10.1016/J.ENERGY.2018.08.001.

Maitra S., Choudhury A., Das H.S., Pramanik M.S.J., C. Technology, A.C.B. Lane, Effect of compaction on the kinetics of thermal decomposition of dolomite under non-isothermal, 0 (2005) 4749–4751. https://doi.org/10.1007/s10853-005-0843-0.

Melia, L., Li, C., Jing, J., Aqsha, A., Shen, B., Chun, A., Loy, M., Lai, B., Chin, F., Shidqi, D., Hameed, N., Guan, G., Sunarso, J., 2021. Bio-oil production from pyrolysis of oil palm biomass and the upgrading technologies : a review. Carbon Resour. Convers. 4, 239–250. https://doi.org/10.1016/j.crcon.2021.10.002.

Miro De Medeiros, A., De, K., Castro, S., Lopes, M., De Macêdo, G., Macêdo, M., Mabel De Morais, A., Ujo, A., Ribeiro Da Silva, D., Gondim, A.D., 2022. Catalytic pyrolysis of coconut oil with Ni/SBA-15 for the production of bio jet fuel. RSC Adv. 12, 10163–10176. https://doi.org/10.1039/D2RA00866A.

Mishra, R.K., Mohanty, K., 2018. Thermocatalytic conversion of non-edible Neem seeds towards clean fuel and chemicals. J. Anal. Appl. Pyrolysis. 134, 83–92. https://doi.org/10.1016/J.JAAP.2018.05.013.

Muhammad, K., Ng, A., Lup, K., Khan, S., Abnisa, F., 2021. Optimization of palm shell pyrolysis parameters in helical screw fluidized bed reactor : effect of particle size, pyrolysis time and vapor residence time. Clean. Eng. Technol. 4, 100174 https://doi.org/10.1016/j.clet.2021.100174.

Mysore Prabhakara, H., Bramer, E.A., Brem, G., 2021. Role of dolomite as an in-situ CO2 sorbent and deoxygenation catalyst in fast pyrolysis of beechwood in a bench scale fluidized bed reactor. Fuel Process. Technol. 224, 107029 https://doi.org/10.1016/J.FUPROC.2021.107029.

Nayab, R., Imran, M., Ramzan, M., Tariq, M., Taj, M.B., Akhtar, M.N., Iqbal, H.M.N., 2022. Sustainable biodiesel production via catalytic and non-catalytic transesterification of feedstock materials – A review. Fuel 328, 125254. https://doi.org/10.1016/j.fuel.2022.125254.

Norouzi, O., Taghavi, S., Arku, P., Jafarian, S., Signoretto, M., 2021. Applied Pyrolysis What is the best catalyst for biomass pyrolysis ? J. Anal. Appl. Pyrolysis. 158, 105280 https://doi.org/10.1016/j.jaap.2021.105280.

Olszak-Humienik, M., Jablonski, M., 2014. Thermal behavior of natural dolomite. J. Therm. Anal. Calorim. 119, 2239–2248. https://doi.org/10.1007/S10973-014-4301-6, 2014 1193.

Prasad, H., Kannapu, R., Pyo, S., Shiung, S., Jae, J., Hoon, G., Ali, M., Jeon, B., Park, Y., 2022. Bioresource Technology MgO-modified activated biochar for biojet fuels from pyrolysis of sawdust on a simple tandem micro-pyrolyzer. Bioresour. Technol. 359, 127500 https://doi.org/10.1016/j.biortech.2022.127500.

Putun, E., 2010. Catalytic pyrolysis of biomass: effects of pyrolysis temperature, sweeping gas flow rate and MgO catalyst. Energy 35, 2761–2766.

Raman S., Zainon Z., Shiong C., Energy consumption trends and their linkages with renewable energy policies in East and Southeast Asian countries : challenges and opportunities, 28 (2018). https://doi.org/10.1016/j.serj.2018.08.006.

Ruddy D.A., Schaidle J.A., Ferrell J.R., Wang J., Moens L., Hensley J.E., Recent advances in heterogeneous catalysts for bio-oil upgrading via "ex situ catalytic fast pyrolysis": catalyst development through the study of model compounds, 2014. https://doi.org/10.1039/c3gc41354c.

Shahruzzaman, R.M.H.R., Ali, S., Yunus, R., Yun-Hin, T.Y., 2018. Green Biofuel Production via Catalytic Pyrolysis of Waste Cooking Oil using Malaysian Dolomite Catalyst. Bull. Chem. React. Eng. Catal. 13, 489–501. https://doi.org/10.9767/BCREC.13.3.1956.489-501.

Sharma, P., Usman, M., Salama, E., Redina, M., Thakur, N., Li, X., 2021. Evaluation of various waste cooking oils for biodiesel production : a comprehensive analysis of feedstock. Waste Manag 136, 219–229. https://doi.org/10.1016/j.wasman.2021.10.022.

Shen, L., Min, F., Liu, L., Zhu, J., Xue, C., Cai, C., Zhou, W., Wang, C., 2019. Application of gaseous pyrolysis products of the waste cooking oil as coal flotation collector. Fuel 239, 446–451. https://doi.org/10.1016/j.fuel.2018.11.056.

Shien, R., Amran, T., Abdullah, T., Azam, S., Zin, R., Isa, K., 2019. ScienceDirect Catalytic steam reforming of complex gasified biomass tar model toward hydrogen over dolomite promoted nickel catalysts. Int. J. Hydrogen Energy. 44, 21303–21314. https://doi.org/10.1016/j.ijhydene.2019.06.125.

Su, G., Chyuan, H., Mofijur, M., Mahlia, T.M.I., Sik, Y., 2022a. Pyrolysis of waste oils for the production of biofuels : a critical review. J. Hazard. Mater. 424, 127396 https://doi.org/10.1016/j.jhazmat.2021.127396.

Su, Z., Jin, K., Wu, J., Huang, P., Liu, L., Xiao, Z., Peng, H., Fan, L., Zhou, W., 2022b. Journal of Analytical and Applied Pyrolysis Phosphorus doped biochar as a deoxygenation and denitrogenation catalyst for ex-situ upgrading of vapors from microwave-assisted co-pyrolysis of microalgae and waste cooking oil. J. Anal. Appl. Pyrolysis. 164, 105538 https://doi.org/10.1016/j.jaap.2022.105538.

Susianti, B., Warmadewanthi, I.D.A.A., Voijant, B., 2022. Bioresource Technology Reports Characterization and experimental evaluation of cow dung biochar + dolomite for heavy metal immobilization in solid waste from silica sand purification. Bioresour. Technol. Reports. 18, 101102 https://doi.org/10.1016/j.biteb.2022.101102.

Syamsiro, M., Saptoadi, H., Norsujianto, T., Noviasri, P., 2014. Fuel Oil Production from Municipal Plastic Wastes in Sequential Pyrolysis and Catalytic Reforming Reactors. Energy Procedia 47, 180–188. https://doi.org/10.1016/j.egypro.2014.01.212.

Tao, L., Huang, J., Dastan, D., Wang, T., Li, J., Yin, X., Wang, Q., 2021. Applied Surface Science New insight into absorption characteristics of CO 2 on the surface of calcite, dolomite, and magnesite. Appl. Surf. Sci. 540, 148320 https://doi.org/10.1016/j.apsusc.2020.148320.

Tsai, W.T., Lee, M.K., Chang, Y.M., 2007. Fast pyrolysis of rice husk: product yields and compositions. Bioresour. Technol. 98, 22–28. https://doi.org/10.1016/J.BIORTECH.2005.12.005.

Valle, B., Aramburu, B., Santiviago, C., Bilbao, J., Gayubo, A.G., 2014. Upgrading of Bio-Oil in a Continuous Process with Dolomite Catalyst. Energy and Fuels 28, 6419–6428. https://doi.org/10.1021/EF501600F.

Valle, B., García-gómez, N., Remiro, A., Bilbao, J., Gayubo, A.G., 2020. Dual catalyst-sorbent role of dolomite in the steam reforming of raw bio-oil for producing H 2 -rich syngas. Fuel Process. Technol. 200, 106316 https://doi.org/10.1016/j.fuproc.2019.106316.

Valle, B., García-Gómez, N., Remiro, A., Gayubo, A.G., Bilbao, J., 2019a. Cost-effective upgrading of biomass pyrolysis oil using activated dolomite as a basic catalyst. Fuel Process. Technol. 195, 106142 https://doi.org/10.1016/J.FUPROC.2019.106142.

B. Valle, A. Remiro, N. García-gómez, A.G. Gayubo, J. Bilbao, Recent research progress on bio-oil conversion into bio-fuels and raw chemicals: a review, (2019). https://doi.org/10.1002/jctb.5758.

Wang, F., Yu, F., Wei, Y., Li, A., Xu, S., Lu, X., 2021a. Promoting hydrocarbon production from fatty acid pyrolysis using transition metal or phosphorus modified Al-MCM-41 catalyst. J. Anal. Appl. Pyrolysis. 156, 105146 https://doi.org/10.1016/J.JAAP.2021.105146.

Wang, P., Shen, Y., 2022. Catalytic pyrolysis of cellulose and chitin with calcined dolomite – Pyrolysis kinetics and products analysis. Fuel 312, 122875. https://doi.org/10.1016/J.FUEL.2021.122875.

Wang, S., Yuan, C., Esakkimuthu, S., Xu, L., Cao, B., El-Fatah Abomohra, A., Qian, L., Liu, L., Hu, Y., 2019a. Catalytic pyrolysis of waste clay oil to produce high quality biofuel. J. Anal. Appl. Pyrolysis. 141, 104633 https://doi.org/10.1016/J.JAAP.2019.104633.

Wang, X., 2019. In-situ High-Temperature XRD and FTIR for Calcite, Dolomite and Magnesite : anharmonic Contribution to the Thermodynamic Propertie. s 30, 964–976.

Wang, Y., Wu, Q., Yang, S., Yang, Q., Wu, J., Ma, Z., Jiang, L., 2019b. Microwave-assisted catalytic fast pyrolysis coupled with microwave- absorbent of soapstock for bio-oil in a downdraft reactor. Energy Convers. Manag. 185, 11–20. https://doi.org/10.1016/j.enconman.2019.01.101.

Wang, Z., Tian, Q., Guo, J., Wu, R., Zhu, H., Zhang, H., 2021b. Co-pyrolysis of sewage sludge /cotton stalks with K 2 CO 3 for biochar production : improved biochar porosity and reduced heavy metal leaching. Waste Manag 135, 199–207. https://doi.org/10.1016/j.wasman.2021.08.042.

Wan Mahari, W.A., Azwar, E., Foong, S.Y., Ahmed, A., Peng, W., Tabatabaei, M., Aghbashlo, M., Park, Y.K., Sonne, C., Lam, S.S., 2021. Valorization of municipal wastes using co-pyrolysis for green energy production, energy security, and environmental sustainability: a review. Chem. Eng. J. 421, 129749 https://doi.org/10.1016/J.CEJ.2021.129749.

Williams, P.T., Nugranad, N., 2000. Comparison of products from the pyrolysis and catalytic pyrolysis of rice husks. Energy 25, 493–513. https://doi.org/10.1016/S0360-5442(00)00009-8.

Wu, Q., Ke, L., Wang, Y., Zhou, N., Li, H., Yang, Q., Xu, J., Dai, L., Zou, R., Liu, Y., Ruan, R., 2022. Pulse pyrolysis of waste cooking oil over CaO: exploration of catalyst deactivation pathway based on feedstock characteristics. Appl. Catal. B Environ. 304, 120968 https://doi.org/10.1016/J.APCATB.2021.120968.

Zhang, G., Liu, H., Wang, J., Wu, B., 2018. Catalytic gasification characteristics of rice husk with calcined dolomite. Energy 165, 1173–1177. https://doi.org/10.1016/J.ENERGY.2018.10.030.

Zhang, J., Liu, J., Liu, R., 2015a. Effects of pyrolysis temperature and heating time on biochar obtained from the pyrolysis of straw and lignosulfonate. Bioresour. Technol. 176, 288–291. https://doi.org/10.1016/j.biortech.2014.11.011.

Zhang, Q., Xu, Y., Li, Y., Wang, T., Zhang, Q., Ma, L., He, M., Li, K., 2015b. Investigation on the esterification by using supercritical ethanol for bio-oil upgrading q. Appl. Energy. 160, 633–640. https://doi.org/10.1016/j.apenergy.2014.12.063.

Zhang, X., Sun, L., Chen, L., Xie, X., Zhao, B., Si, H., 2014. Journal of Analytical and Applied Pyrolysis Comparison of catalytic upgrading of biomass fast pyrolysis vapors over CaO and Fe (III)/CaO catalysts. J. Anal. Appl. Pyrolysis. 108, 35–40. https://doi.org/10.1016/j.jaap.2014.05.020.

Zhou, X., Li, X., Zhao, B., Chen, X., Zhang, Q., 2022. Discriminant analysis of vegetable oils by thermogravimetric-gas chromatography /mass spectrometry combined with data fusion and chemometrics without sample pretreatment. LWT 161, 113403. https://doi.org/10.1016/j.lwt.2022.113403.

Zhu H., Yao Y., Wang R., Comparative Study of the Effects of Various Activation Methods on the Desulfurization Performance of Petroleum Coke, 21 (2020) 1–14.